Research Paper

Sound Field Modelling and Noise Reduction for a Forklift Power Compartment Based on Perfectly Matched Layer and Acoustic Packaging Design

Enlai ZHANG[(1),(2)*], Zhiqi LIU[(2)], Jingjing ZHANG[(3)], Jiahe LIN[(4)]

[(1)] *School of Mechanical and Automotive Engineering, Xiamen University of Technology*
Xiamen, China
[*]Corresponding Author e-mail: zhangenlai1986@163.com

[(2)] *Chengyi University College, Jimei University*
Xiamen, China

[(3)] *College of Applied Science and Technology, Hainan University*
Danzhou, China

[(4)] *Department of Mechanical and Electrical Engineering, Xiamen University*
Xiamen, China

(*received December 19, 2019; accepted June 10, 2021*)

The core goal of this paper is to put forward a feasible scheme of noise reduction for a target forklift on the basis of solving the problem of vibration and acoustic radiation from complex structures in infinite domain. Based on the previous report and vibration acceleration tests, the acoustic virtual wind tunnel model of forklift power compartment was established using finite element method and boundary element method, in which the perfectly matched layer was first applied to simulate the attenuation propagation of sound waves in air. In addition, according to the distribution characteristics of sound pressure field with different frequencies, the acoustic energy mainly radiated through the bottom and right side, and concentrated in the low frequency. Consequently, the acoustic packaging design for the whole forklift power compartment was presented, and a satisfying noise reduction effect was achieved.

Keywords: forklift power compartment; sound field modelling; perfectly matched layer; acoustic packaging design; noise reduction.

1. Introduction

Currently noise has become an important index to measure the performance of engineering vehicles (Zhang *et al.*, 2021). It is of great engineering significance to study the mechanism of vibration and acoustic radiation for noise reduction. However, for most engineering application problems, the acoustic radiation caused by structural vibration is difficult to be solved analytically. The physical model commonly used has three forms: partial differential equation; integral form on a certain region and integral form on the boundary (Dammak *et al.*, 2019; Bi *et al.*, 2018; Chen *et al.*, 2019; Lock, Holloway, 2016). These mathematical forms are theoretically equivalent, but are not equivalent in practical applications, thus forming corresponding physical modeling methods, i.e. finite difference method (FDM), finite element method (FEM) and boundary element method (BEM). Among them, FEM applied to the acoustic analysis is to first mesh sound field, establish a finite element discrete model according to the acoustic wave equation and the required boundary condition, and then the results describing the distribution of sound field and the characteristics of acoustic radiation can be obtained by acoustic solution (Gao *et al.*, 2018; Tian *et al.*, 2017). For example, Kolber *et al.* (2014) used Hashimoto's discrete calculation method (Hashimoto, 2001), which is a hybrid

method including vibration measurement and radiation impedance calculation, to determine the acoustic radiation efficiency and analyze the influence of the discrete degree and the parameters of different geometric structure measuring devices on the measurement accuracy. Furthermore, Kozien (2009; 2005) proposed a hybrid method using FEM to estimate the radiated sound, which can promote the discretization analysis on the sound field.

However, FEM mainly exists in the process of simulating and calculating the acoustic radiation, and the numerical solution is difficult, in particular, the shortage of the cut-off edge of the acoustic radiation cannot be divided. The deficiency of the FEM can be made up by the BEM, and BEM is to discretize boundary conditions in the solution domain and obtain the function value by the boundary integral equations (Gao *et al.*, 2019; Chen *et al.*, 2017).

Chen and Schweikert (1963) applied BEM to the acoustic field for the first time. They derived a series of integral equations through sound field distribution and proposed an acoustic radiation prediction method in infinite space. Subsequently, many scholars have done extensive research on BEM (Chen *et al.*, 2016; Liu *et al.*, 2017), and its applicability was extended to the irregular structure. In the practical application, FEM and BEM are generally combined to solve the vibration and acoustics problems (Gao *et al.*, 2019; Chen *et al.*, 2017; Jang *et al.*, 2013; Loeffler *et al.*, 2015), and the advantages of both are fully exploited, that is, the finite element is adapted to the complex geometry, and the boundary element can solve the problem of the acoustic radiation in the infinite field. In this paper, the numerical method based on FEM-BEM is applied to establish a virtual model of the vibration and acoustic radiation from a forklift power compartment, and to calculate the sound field distribution and explore the experimental investigation on noise reduction.

2. Model of sound field generated by vibrating structures

In this section, a forklift power compartment was taken as the research object. Acceleration parameters were obtained through vibration test of structures from main noise sources, and the perfectly matched layer (PML) was introduced to establish a non-reflective acoustic model of the whole forklift power compartment in the air domain, and simulation calculation and analysis were carried out.

2.1. General idea and implementing of PML

The complex internal structure system of forklift power compartment includes engine, intake and exhaust, cooling fan and heat dissipation etc., as illustrated in Fig. 1. Since the sound waves radiated from the structural surfaces of the power compartment are directly diffused in the air, it is necessary to establish an air domain outside the solid domain to calculate the distribution of the sound field in the air. In the published reports (Komatisch, Tromp, 2003; Bermudez *et al.*, 2014; Duru, Kreiss, 2014) PML was utilized to simulate the attenuation and reflection-free propagation of sound waves in the computational domain. In order to improve the computational efficiency, internal components of forklift power compartment, such as tubings, screws and pin shafts, were simplified, and an acoustics virtual wind with air domain including PML was established. Its 3D physical model and mesh model are shown in Figs. 2 and 3, respectively.

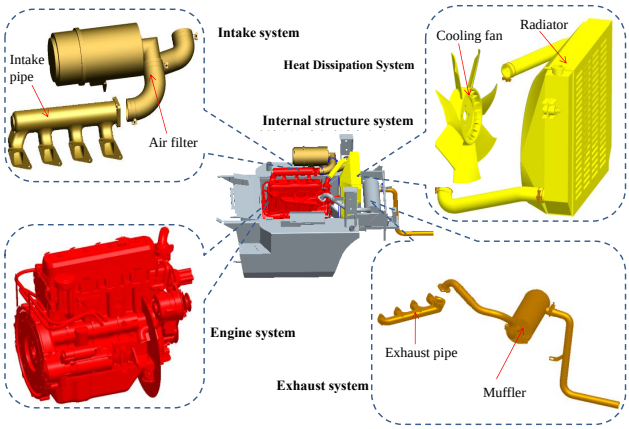

Fig. 1. Internal composition of the forklift power compartment.

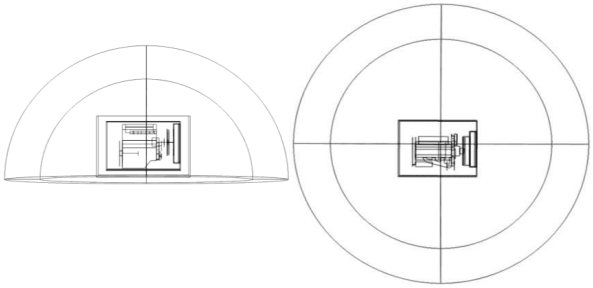

Fig. 2. 3D physical model of the virtual wind tunnel.

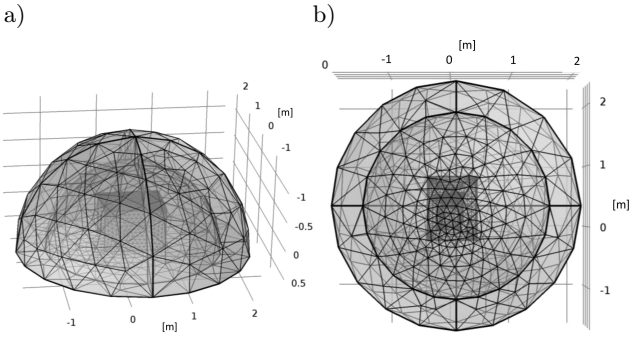

Fig. 3. Mesh model of the virtual wind tunnel.

It should be noted that the mesh division and numerical calculation are performed in COMSOL Multiphysics software, which is based on partial differential equations to solve the interaction between physical fields (Dogan *et al.*, 2018; Qu *et al.*, 2019). Under the continuous condition between the normal vibration acceleration and the sound pressure, sound sources can be approximately calculated by the structure surface particles. Derived from COMSOL, the governing equation describing the normal acceleration of surface vibration and radiation sound pressure is expressed as:

$$-\mathbf{n}\cdot\left(-\frac{1}{\rho}(\nabla p - q)\right) = \mathbf{a}_n, \tag{1}$$

where $\mathbf{n}$ is the unit normal vector pointed outside the solid domain; ρ is the density; p is the sound pressure; q represents a dipole source that can describe the reflection of sound waves against structural obstacles; $\mathbf{a}_n$ is the initial acceleration of structural surface vibration and ∇ is the divergence operator.

That is to say, after obtaining the vibration acceleration of component surface from the power compartment, the main noise sources can be set and simulated in COMSOL by Eq. (1), and the setting content mainly includes the structure surface, acceleration amplitude and its direction. In particular, when the other surfaces are hard acoustic field boundary conditions, namely the walls, their normal accelerations are set as zero (i.e. $\mathbf{a}_n = 0$).

Previous researches indicated that the radiation noise sources of the forklift power compartment at idle speed mainly came from the engine body, intake and exhaust systems (Zhang *et al.*, 2015). It should be pointed out that sound sources in the acoustic simulation were set by the surface vibration acceleration applied on engine body, exhaust pipe, intake pipe and other structures, and these settings were directly performed in COMSOL, including the choice of corresponding geometric surfaces, the magnitude and direction of acceleration. To obtain the surface acceleration information, the vibration tests under idle condition were conducted, and the surface vibration acceleration signals were extracted by sensors. The tested prototype run at idle speed, and the vibration acceleration was collected when the whole machine reached a stable state. The acceleration frequency characteristics of measuring points were analyzed. And the results are illustrated in Fig. 4.

Figure 4 shows that there are peaks of vibration acceleration on the engine surface, exhaust pipe and intake pipe, corresponding to 1.45 m/s^2, 2.51 m/s^2, and 1.226 m/s^2, respectively. Moreover, the peak accelerations of the engine surface and exhaust pipe are relatively obvious.

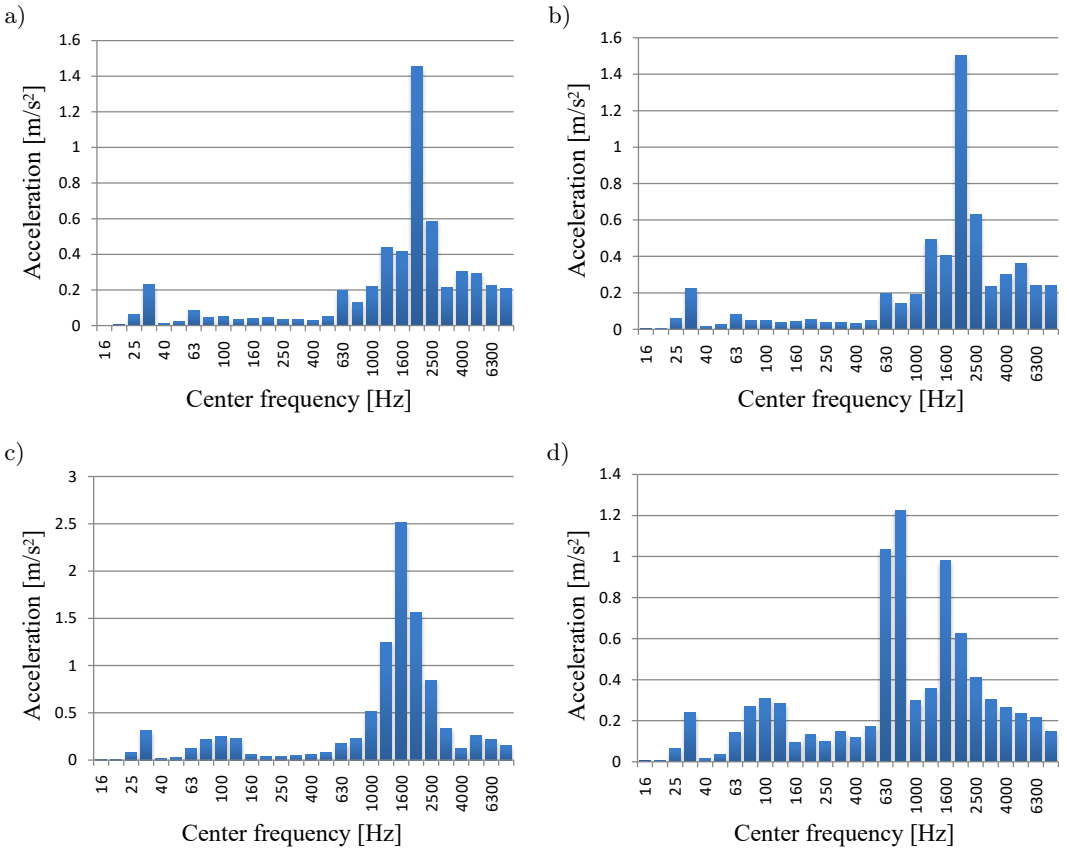

Fig. 4. Vibration acceleration tests of each measuring point:
a) engine surface 1, b) engine surface 2, c) exhaust pipe, d) intake pipe.

2.2. Calculation results

Based on the simplified geometric model and the boundary analysis of the physical field, the experimental data were set to the corresponding boundary conditions of sound sources. In COMSOL, define global parameters, including surface accelerations, structural geometric parameters etc., import the simplified three-dimensional geometric model, establish the virtual wind tunnel model (i.e. air computing domain), and define "perfectly matched layer" to simulate the acoustic radiation in atmospheric space. The Helmholtz boundary integral equation of structural vibro-acoustic radiation was solved by "pressure acoustics, frequency domain" interface, and the "internal normal acceleration" boundary was added to simulate the sound sources and the "internal hard sound field (wall)" boundary was also added to simulate the acoustic reflection of the structure wall. The frequency calculation range was set as 10 to 1000 Hz, and due to limited space, the numerical calculation results of sound field distribution of typically selected 6 characteristic frequencies were presented, as shown in Fig. 5.

Figure 5 indicates that the power compartment has different sound pressure distribution characteristics at different frequencies. With the increase of frequency, the total sound pressure increases first and then decreases as a whole, that is, the maximum sound pressure of 50 Hz is 0.14 Pa and 1.35 Pa more than that of 30 Hz and 810 Hz, respectively. Obviously, the ma-

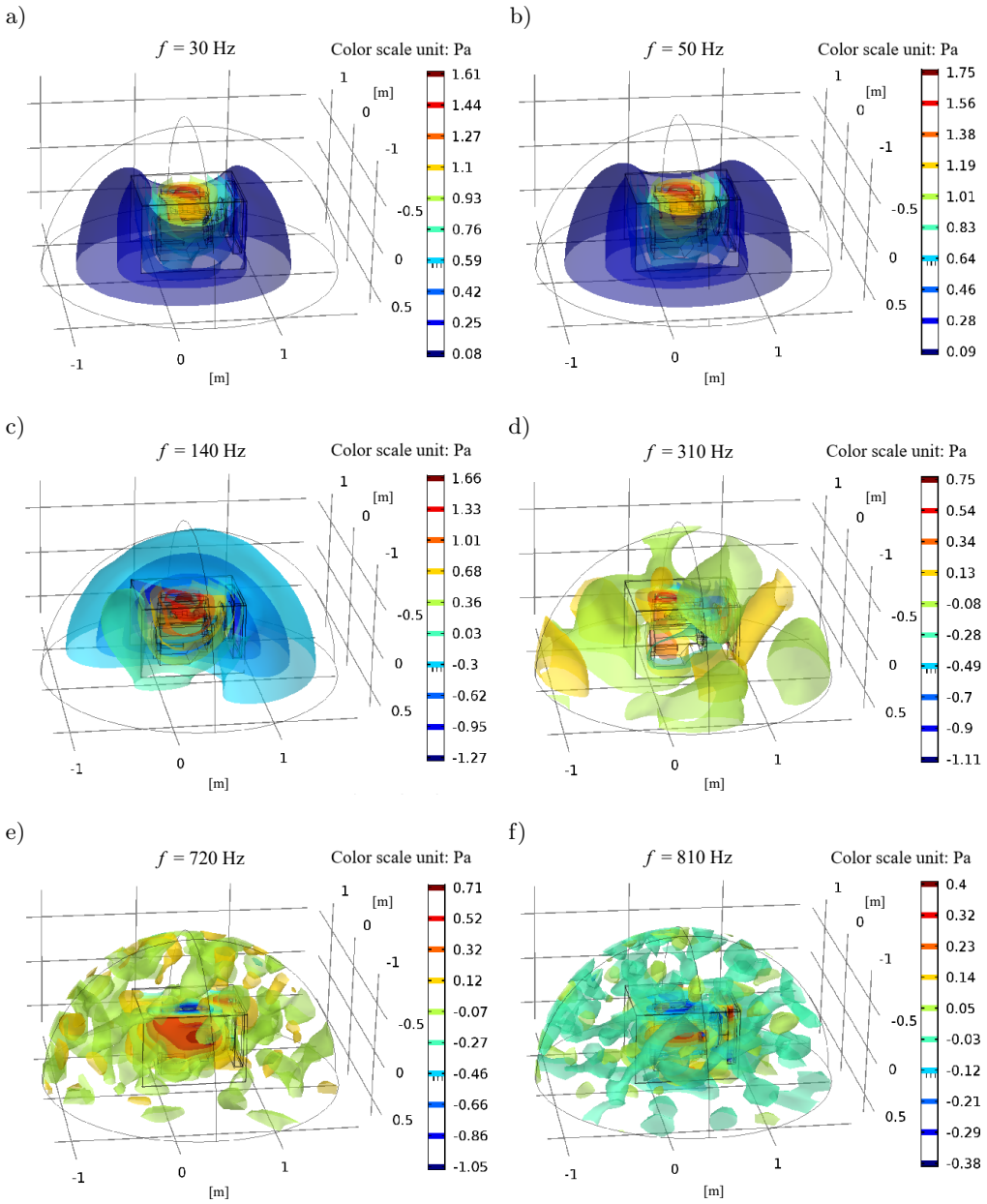

Fig. 5. Distribution of total sound pressure field in power compartment with different frequencies.

ximum sound pressure is more likely to occur at low frequencies. In addition, the distribution of sound field is obviously directional, and the maximum sound pressure is mainly concentrated in the geometric structure of the engine radiating sound waves outwardly from the starting point of the main sound source, attenuating and disappearing in the computational domain of PML, which is consistent with the actual sound radiation characteristics.

3. Noise reduction

3.1. Scheme of acoustic packaging design

As the above acoustic energy is mainly concentrated in low frequency, the noise reduction scheme is mainly aimed at low frequency noise. Passive noise reduction measures are adopted in this paper, which involves the distribution of acoustic radiation and its spectrum characteristics. In order to obtain the sound field distribution of low frequency noise more intuitively, the first three sound field distributions from Fig. 5 were sectioned. The results are shown in Fig. 6.

Figure 6 demonstrates that the low-frequency sound pressure radiates outwardly from the bottom and right side, which is consistent with the previous research results (Zhang *et al.*, 2015). Consequently, the acoustic packaging design was carried out for the forklift power compartment, and the improved positions were marked with yellow and orange, as shown in Fig. 7. A reserved space is located between the two improved positions, the purpose of which is to ensure

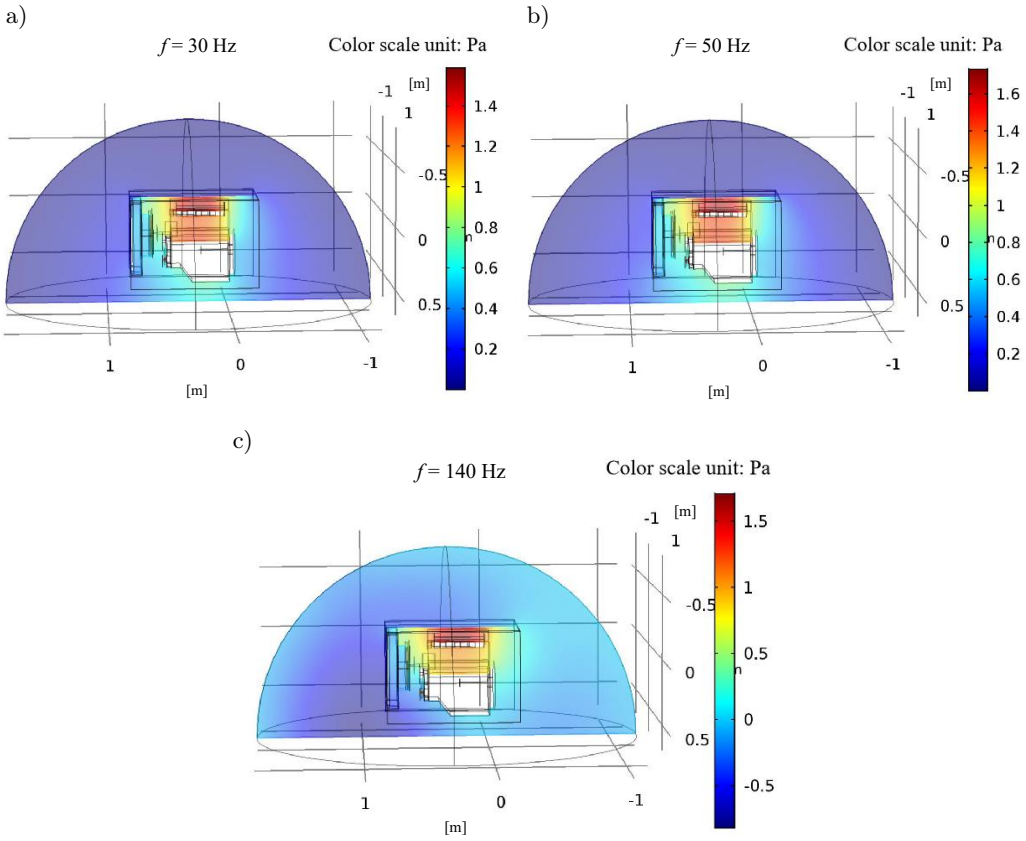

Fig. 6. Three low-frequency sections of the sound field.

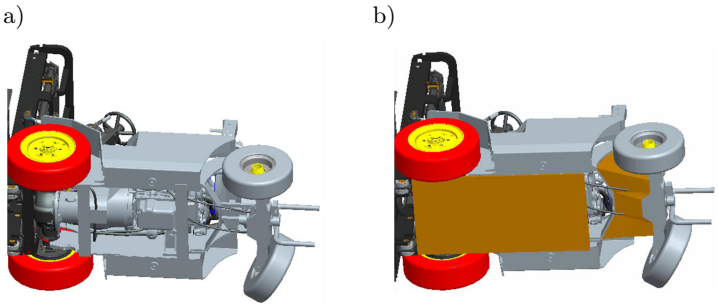

Fig. 7. Scheme of acoustic packaging: a) before improvement, b) after improvement.

the circulation and heat dissipation of air flow in the power compartment. In recent years, due to internal damping viscoelasticity, polymer composites have been widely applied in the field of low-frequency sound absorption. For example, as reported (Mott *et al.*, 2002), the relationship between damping properties of rubber plastic composite material (RPCM) has been studied by standing wave tube experiment; in addition, butyl rubber damping plate (BRDP) has the advantages of low cost and easy realization, and has been widely used in sound insulation, especially for reducing vehicle low-frequency noise (Yang, 2013). It should be pointed out that relevant studies show that the combination of sound absorption and sound insulation materials can give more obvious noise reduction effect (Cai *et al.*, 2010). Therefore, in this case, the RPCM with the thickness of 3 cm combined with BRDP was utilized to conduct acoustic packaging for the targeted forklift power compartment, as illustrated in Fig. 8.

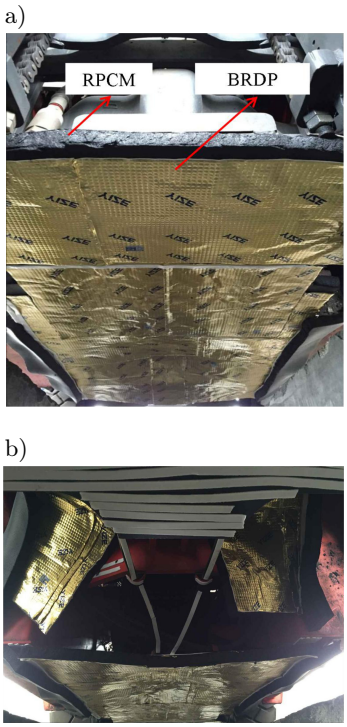

Fig. 8. Composite materials are distributed at the bottom and right side in the forklift engine compartment, as shown in (a) and (b), respectively (Zhang *et al.*, 2018).

3.2. Improved test and noise reduction effect

According to the forklift industry standard of JB/T 3300-2010, the radiated noise signals of the targeted forklift before and after the improvements were respectively tested under three standard working conditions, namely lifting, running and idling. The test results are shown in Fig. 9, from which it can be seen that the radiation sound pressure level of each working condition after improvement is reduced, and the total sound

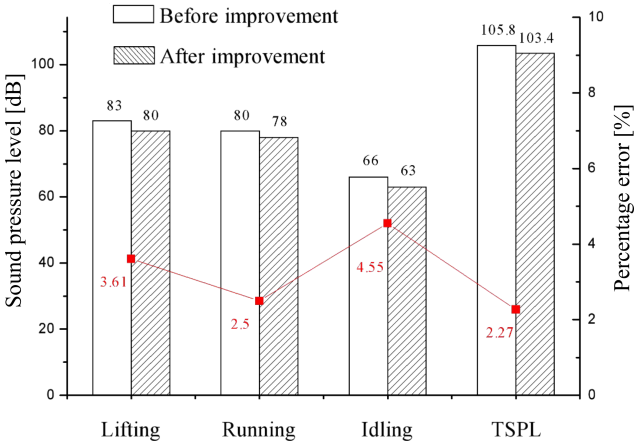

Fig. 9. Comparison of noise reduction before and after improvements.

power level has decreased from 105.8 dB to 103.4 dB, which meets the standard limit of 104 dB in the industry when the rated engine power is 40 kW.

4. Conclusions and future work

This paper applied PML to explore the non-reflective acoustic modelling method of a forklift power compartment. Through vibration acceleration test and previous research results, a virtual wind tunnel model was successfully established in COMSOL to simulate the propagation of sound waves from forklift power compartment in the air, and numerical calculations were carried out to obtain sound field distribution at different frequencies. According to the section analysis in the low frequency sound field distribution which was the main source of radiated acoustic energy, the acoustic packaging design scheme was put forward. And the noise reduction effect is to meet the requirement of forklift industry, which further demonstrates the feasibility of using PML in this case to establish the acoustic model and the effectiveness of the acoustic packaging scheme. Additionally, further work on the targeted forklift is to analyze the spectral characteristics between structural vibration and radiation noise, and compare the acoustic characteristics of different materials to obtain better noise reduction effect.

Acknowledgments

The work was supported by National Natural Science Foundation of China (12004136), Xiamen Youth Innovation Foundation (3502Z20206024), Key Project of Research and Development in Hainan Province (ZDYF2020038), Doctoral Scientific Research Foundation of Chengyi University College (CK17063), and Outstanding Young Scientific Research Talents Cultivation Plan of Fujian Universities (ZX19033).

References

1. Bermudez A., Hervella-Nieto L., Prieto A., Rodriguez R. (2014), An optimal perfectly matched layer with unbounded absorbing function for time-harmonic acoustic scattering problems, *Journal of Computational Physics*, **223**(2): 469–488, doi: 10.1016/j.jcp.2006.09.018

2. Bi C.X., Zhang Y., Zhang X.Z., Zhang Y.B. (2018), Stability analysis of inverse time domain boundary element method for near-field acoustic holography, *The Journal of the Acoustical Society of America*, **143**(3): 1308–1317, doi: 10.1121/1.5026024.

3. Cai H,S., Li X.X., Zhang W.B. (2010), Analysis and experimental study on sound absorption and noise reduction performance of some composite materials, *Noise and Vibration Control*, **4**: 54–57, doi: 10.3969/j.issn.1006-1355.2010.04.015.

4. Chen L.H., Schweikert D.G. (1963), Sound radiation from an arbitrary body, *The Journal of the Acoustical Society of America*, **35**(10): 1626–1632, doi: 10.1121/1.1918770.

5. Chen L.L., Liu L.C., Zhao W.C., Chen H.B. (2016), 2D acoustic design sensitivity analysis based on adjoint variable method using different types of boundary elements, *Acoustics Australia*, **44**(2): 343–357, doi: 10.1007/s40857-016-0065-4.

6. Chen L.L., Zhao W.C., Liu C., Chen H.B. (2017), 2D structural acoustic analysis using the FEM/FMBEM with Different Coupled Element Types, *Archives of Acoustics*, **42**(1): 37–48, doi: 10.1515/aoa-2017-0005.

7. Chen L.L., Zhao W.C., Liu C., Chen H.B., Marburg S. (2019), Isogeometric Fast Multipole Boundary Element Method based on Burton-Miller formulation for 3D acoustic problems, *Archives of Acoustics*, **44**(3): 475–492, doi: 10.24425/aoa.2019.129263.

8. Dammak K., Koubaa S., EI Hami A., Walha L., Haddar M. (2019), Numerical modelling of vibro-acoustic problem in presence of uncertainty: Application to a vehicle cabin, *Applied Acoustics*, **144**: 113–123, doi: 10.1016/j.apacoust.2017.06.001.

9. Dogan H., Eisenmenger C., Ochmann M. (2018), A LBIE-RBF solution to the convected wave equation for flow acoustics, *Engineering Analysis with Boundary Elements*, **92**: 196–206, doi: 10.1016/j.enganabound.2017.11.016.

10. Duru K., Kreiss G. (2014), Efficient and stable perfectly matched layer for CEM, *Applied Numerical Mathematics*, **76**: 34–47, doi: 10.1016/j.apnum.2013.09.005.

11. Gao K., Fu S.B., Chung E.T. (2018), A high-order multiscale finite-element method for time-domain acoustic-wave modeling, *Journal of Computational Physics*, **360**: 120–136, doi: 10.1016/j.jcp.2018.01.032.

12. Gao R.X., Zhang Y.H., Kennedy D. (2019), Topology optimization of sound absorbing layer for the mid-frequency vibration of vibro-acoustic systems, *Structural and Multidisciplinary Optimization*, **59**(5): 1733–1746, doi: 10.1007/s00158-018-2156-3.

13. Hashimoto N. (2001), Measurement of sound radiation efficiency by the discrete calculation method, *Applied Acoustics*, **62**(4): 429–446, doi: 10.1016/S0003-682X(00)00025-6.

14. Jang H.W., Ih J.G. (2013), On the instability of time-domain acoustic boundary element method due to the static mode in interior problems, *Journal of Sound and Vibration*, **332**(24): 6463–6471, doi: 10.1016/j.jsv.2013.07.018.

15. Kolber K., Snakowska A., Kozupa M. (2014), The effect of plate discretizationon accuracy of the sound radiation efficiency measurements, *Archives of Acoustics*, **39**(4): 511–518, doi: 10.2478/aoa-2014-0055.

16. Komatisch D., Tromp J. (2003), A perfectly matched layer absorbing boundary condition for the second-order seismic wave equation, *Geophysical Journal International*, **154**(1):146–153, doi: 10.1046/j.1365-246X.2003.01950.x.

17. Kozien M.S. (2005), Hybrid method of evaluation of sounds radiated by vibrating surface elements, *Journal of Theoretical and Applied Mechanics*, **43**(1): 119–133.

18. Kozien M.S. (2009), Acoustic intensity vector generated by vibrating set of small areas with random amplitudes, *Journal of Theoretical and Applied Mechanics*, **47**(2): 411–420.

19. Liu X.J., Wu H.J., Jiang W.K. (2017), A boundary element method based on the hierarchical matrices and multipole expansion theory for acoustic problems, *International Journal of Computational Methods*, **15**: 1850009, doi: 10.1142/S0219876218500093.

20. Lock A., Holloway D. (2016), Boundary element modelling of a novel simple enhanced bandwidth schroeder diffuser offering comparable performance to a fractal design, *Acoustics Australia*, **44**(1): 137–147, doi: 10.1007/s40857-016-0049-4.

21. Loeffler C.F., Mansur W.J., Barcelos H.D., Bulcao A. (2015), Solving Helmholtz problems with boundary element method using direct radial basis function interpolation, *Engineering Analysis with Boundary Elements*, **61**: 218–225, doi: 10.1016/j.enganabound.2015.07.013.

22. Mott P.H., Michael R.C., Corsaro R.D. (2002), Acoustic and dynamic mechanical properties of a polyurethane rubber, *The Journal of the Acoustical Society of America*, **111**(4): 1782–1790, doi: 10.1121/1.1459465.

23. Qu W.Z., Fan C.M., Gu Y., Wang F.J. (2019), Analysis of three-dimensional interior acoustic fields by using the localized method of fundamental solu-

tions, *Applied Mathematical Modelling*, **76**: 122–132, doi: 10.1016/j.apm.2019.06.014.

24. Tian W.Y., Yao L.Y., Li L. (2017), A Coupled Smoothed Finite Element-Boundary Element Method for structural-acoustic analysis of shell, *Archives of Acoustics*, **42**(1): 49–59, doi: 10.1515/aoa-2017-0006.

25. Yang H.B. (2013), Low-frequency acoustic absorption mechanism of a viscoelastic layer with resonant cylindrical scatterers, *Acta Physica Sinca*, **62**(15): 223–229, doi: 10.7498/aps.62.154301.

26. Zhang E.L., Hou L., Yang W.P. (2015), Noise source identification and experimental research of engine compartment of a Forklift based on fast independent component analysis and Scan & Paint, *Proceedings of the ASME 2015 International Mechanical Engineering Congress and Exposition*, *Vol. 13: Vibration, Acoustics and Wave Propagation*, Houston, Texas, USA, November 13–19, 2015, doi: 10.1115/IMECE2015-51380.

27. Zhang E.L., Zhang Q.M., Xiao J.J., Hou L., Guo T. (2018), Acoustic comfort evaluation modeling and improvement test of a forklift based on rank score comparison and multiple linear regression, *Applied Acoustics*, **135**: 29–36, doi: 10.1016/j.apacoust.2018.01.026.

28. Zhang E.L., Zhuo J.M., Hou L., Fu C.H., Guo T. (2021), Comprehensive annoyance modeling of forklift sound quality based on rank score comparison and multi-fuzzy analytic hierarchy process, *Applied Acoustics*, **173**: 107705, doi: 10.1016/j.apacoust.2020.107705.